Available online at www.sciencedirect.com
ScienceDirect
Polymer Degradation and Stability 92 (2007) 1213–1218
Polymer Degradation and Stability
www.elsevier.com/locate/polydegstab

Early detection of degradation in a semi-crystalline polyolefin by a successive self-nucleation and annealing technique

C.J. Pérez*, J.M. Carella

Instituto de Investigaciones en Ciencia y Tecnología de Materiales (INTEMA) (UNMdP-CONICET), Facultad de Ingeniería, Universidad Nacional de Mar del Plata, Juan B. Justo 4302, (7600) Mar del Plata, Argentina

Received 2 March 2007; received in revised form 28 March 2007; accepted 3 April 2007
Available online 14 April 2007

Abstract

Samples taken from a black pipeline liner that became fragile while in service were analyzed by a Successive Self-Nucleation and Annealing (SSA) technique. Two types of polyethylene, Low-Density Polyethylene (LDPE) and Linear Low-Density Polyethylene (LLDPE) were aged in air, at several temperatures, and changes in the molecular structure were followed simultaneously by infrared and calorimetric techniques. Samples with and without antioxidants were prepared, aged, and evaluated for the same oxidative treatments. The LDPE type was chosen to be identical to the black LDPE originally used for making the pipeline liner. Oxidative reactions of LDPE and LLDPE were quantified via carbonyl group concentrations measured by FTIR. Changes in the crystallization behavior of the original and aged polymers, and of the black pipeline liner, were monitored via the SSA technique. Changes of the fraction of lamellae of specific thickness in the crystallized polymer could be correlated linearly with the formation of carbonyls, and thus this calorimetric method is proposed to be suitable as a tool for early quantitative monitoring of LDPE degradation.

Keywords: LDPE; Thermal aging; Annealing; Morphology changes

1. Introduction

Polyolefins like polyethylene, polypropylene and several types of their copolymers are widely used as external protective liners for steel pipeline protection. The purpose of using these liners may be mechanical protection, reduction of the corrosion rate by restricting the access of oxygen and moisture to the pipe's external surface, and thermal insulation. For all these purposes, full mechanical integrity of the liners is crucial. Even small cracks developed in fragile liners may permit the access of oxygen and moisture to the steel pipe surface, causing considerable localized damage by corrosion processes. Large cracks developed in liners used for thermal insulations can dramatically increase undesirable heat transfer in oil pipelines placed under the sea [1–5].

Polyolefin liners must be able to deform beyond their yield point without any failure, and this property must remain unchanged for the extent of their expected useful life. Being the values of their thermal expansion coefficients much larger than those for steel, all temperature changes impose large strains to the polymer. Small extents of degradation of the hydrocarbon main chain may well cause large changes in their toughness, since the polyolefin amorphous regions are much more susceptible to oxygen attack, and therefore chain scissions reduce the number of mechanical connections between crystalline lamellae. Detecting these early degradation processes becomes very important for the purpose of modeling to accurately predict liners useful life, and also for monitoring the evolution of pipelines in service.

Thermal and thermo oxidative degradation of polyethylene involves complex reactions that are influenced by many factors: oxygen pressure, temperature, sample thickness, supermolecular structure, antioxidant content, etc [6–9]. Hydrocarbon chain's oxidation produces structures that absorb

* Corresponding author.
E-mail address: cjperez@fi.mdp.edu.ar (C.J. Pérez).

0141-3910/$ - see front matter © 2007 Elsevier Ltd. All rights reserved.
doi:10.1016/j.polymdegradstab.2007.04.004

large amounts of IR energy [10–14], and for this reason sensitive spectroscopic techniques like FTIR have been historically preferred to monitor thermal and oxidative degradation of polyolefin. For the case of pipeline liner formulations the FTIR technique is very difficult to use in the transmission mode, because of the presence of carbon black, and more elaborated techniques need to be used, like ATR mode [15–17]. Carbon black is usually added to polyolefin formulations for protection against UV radiation and also to act as a long-term antioxidant.

In this work we explore the feasibility of using a calorimetric technique to monitor and quantify early stages of polyolefin chain scission. Calorimetric techniques require very small amounts of sample that can be conveniently extracted from the pipelines without causing any damage, and are not affected by the presence of usual amounts of carbon black.

Two types of polyolefin, LDPE and LLDPE, were exposed to atmospheric oxygen for a range of time intervals, at temperatures between 45 and 90 °C, to encompass the higher service temperatures for pipelines and higher, for shorter degradation times and later extrapolation to lower service temperatures. Representative samples were analyzed by the SSA technique that involves the sequential application of self-nucleation and annealing steps to the sample [18–21]. The crystalline lamellae population thus obtained shows a discrete distribution of lamellae thickness that correspond to melting temperatures located just above the annealing temperatures. The SSA technique can be considered as a selective fractionation of crystallizable sequences lengths of polymethylene sequence lengths, because the annealing step allows enough time for diffusion and growth of lamellae. A final heating run reveals the melting of the crystalline populations induced by the previous treatment. Lamellae population thicknesses and relative amounts were calculated from the SSA results by standard methods. It was observed that the relative changes in populations of lamellae of specific thickness can be linearly correlated with the amount of carbonyl groups measured by FTIR, and the technique allows simple detection of chain's scission in the same low range as FTIR does.

Small samples were taken from a black pipeline liner that developed fragility while being in service at normal ambient temperatures, and analyzed by the SSA technique. Comparison of results with those obtained for this study indicates that main chain oxidative scission caused the loss of toughness for the black pipeline liner.

2. Experimental

2.1. Materials and sample preparation

Two types of polyethylene were used in this study. LDPE (203M) and LLDPE (1045.11B) were supplied by Dow-PBB Polisur (Bahía Blanca, Argentina). Two sets of samples of each type of polyethylene were used, that differ only on the amount of antioxidant contained.

About 100 g of each polymer were dissolved in boiling xylene, and quickly precipitated in cool methanol to obtain a fine powder. Most of the antioxidant and other additives are expected to remain in the thus formed xylene–methanol solution. The precipitated polymers were exhaustively dried at room temperature. Samples prepared from polymers stripped by this procedure are identified as LDPE-AF and LLDPE-AF.

Four different types of samples were molded in the form of 0.4 mm thick sheets, by compression molding at 170 °C. Specimens of about 2 g were put in Petri dishes and aged in air at constant temperature in specially designed ovens at 45, 60, 75 and 90 °C, for up to 45 days. Small samples were taken from each specimen once a week, for SSA and FTIR analyses.

Samples taken from the black pipeline liner were analyzed by SSA technique only, as received.

2.2. Evaluation of basic thermal behavior

Small discs (approximately 10 mg) were cut from all original and degraded materials. The discs were encapsulated in DSC aluminum pans. Ultra-high purity dry nitrogen was used as an inert atmosphere for conditioning and tests in a Perkin–Elmer DSC Pyris-2 calorimeter. DSC cooling and heating runs were performed between 25 and 160 °C at a heating rate of 10 °C/min, after the samples were held at 160 °C for 5 min, for standard characterization.

2.3. Successive self-nucleation and annealing (SSA)

The SSA technique consists of successive heating and cooling cycles. The self-nucleation and annealing temperatures (T_s) were chosen by the procedure described by Fillon et al. [22]. A first cycle based on heating and holding in the melt at 160 °C for 5 min, was performed to erase all previous thermal history. Then, each sample was cooled down to 40 °C at 10 °C/min. Another heating scan followed, at the same heating rate, up to the highest of a series of selected self-seeding temperatures denoted as T_s, where the sample was kept for 5 min before cooling it again down to 70 °C at 10 °C/min. The highest value for T_s was always placed 12 °C above the peak melting point for the sample being studied. After that, the sample was heated once again up to a temperature 6 °C below T_s and held there for 5 min. The crystals not melted at this temperature are annealed, some of the melted species crystallize isothermally, and the remaining molten crystallizable chains will only crystallize during the subsequent cooling. This cyclic procedure is repeated by heating the sample at a temperature 6 °C lower than that of the previous annealing, until a heating temperature close to 80 °C is reached. The melting behavior of the samples thus prepared was recorded at a heating rate of 10 °C/min. The T_s range used for LDPE was 77–131 °C and for LLDPE was 83–143 °C.

2.4. Fourier transform infrared spectroscopy

A Mattson FT-IR (Genesis II) instrument was used. The absorbance IR spectra were recorded in the 4000–600 cm^{-1} range with a resolution of 2 cm^{-1}, with 64 scans for each spectrum. FTIR has been used by other authors to study the

carbonyl concentration, in the form of the usual carbonyl index [13,23,24].

A calibration curve was obtained by experimental measurements of the carbonyl absorbance at 1720 cm^{-1} for diluted solutions of behenic acid ($C_{22}H_{44}O_2$) in paraffin. Carbonyl concentrations are used throughout this work, instead of carbonyl index values, for the purpose of reporting quantitative results.

Thin foils about 0.1 mm thick were prepared from the samples under study by compression molding, and IR spectra were measured in the solid state.

3. Results and discussion

Figs. 1–3 show the final DSC melting runs after applying the SSA fractionation technique to the polymers under study. Each peak in the DSC output graph corresponds to the melting of crystals with different lamellar thickness and the whole set gives some information about the molecular structure of each polymer. Samples made out of LDPE show a narrower range of melting temperatures and lamellae thickness than those made out of LLDPE, because of the more uniform distribution of tertiary carbons along the LDPE main chains. Thicker and more stable crystals are formed first, at higher temperatures, whereas other chain segments can form less stable crystals or remain in the molten state and crystallize during the cooling. Only those temperatures capable of producing self-nucleation and annealing (T_s) are reported in Tables 1 and 2, since they are directly responsible for the annealed crystals that subsequently melt during the final heating run shown in Figs. 1–3. The melting points (T_m) of all the lamellae populations produced per sample are associated with the corresponding T_s value, and therefore do not change appreciably along the degradation process. A qualitatively different behavior is observed for polyolefins that undergo crosslinking, where some melting peaks are observed to shift to lower temperature values as the process increasingly restricts the chain mobility [25,26]. On the other hand, area fractions under each peak change continuously, as can be seen in Figs. 1–3 and Table 1. Area fraction changes indicate changes in the amount of uninterrupted crystallized polymethylene sequences of a particular length range.

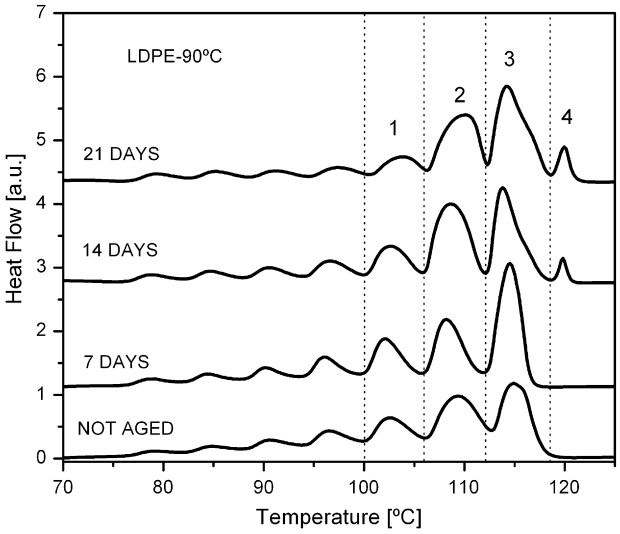

Fig. 2. DSC melting runs for LDPE-AF for several values of aging time, at 90 °C.

Fig. 1 shows the final DSC melting runs for LDPE-AF after 21 days of aging at three different temperatures. As expected, higher temperatures increase the degradation reaction rates shown as changes in the DSC melting traces. The most noticeable changes are observed for the peaks labeled 1, 2, 3 and 4. For these relatively short times, the area fractions corresponding to peak 3 increase by almost 100% when aged at 90 °C. The increase of the area fraction corresponding to peak 3 indicates corresponding increase in the weight fraction of the longer polymethylene sequences available for crystallization.

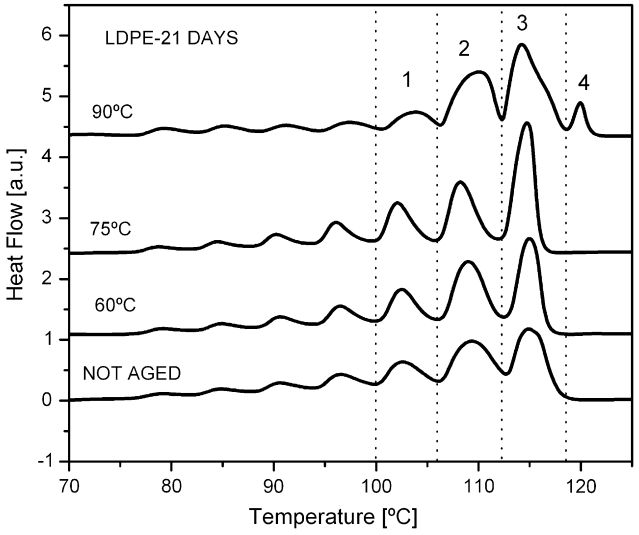

Fig. 1. DSC melting runs for LDPE-AF after 21 days of aging at three different temperatures.

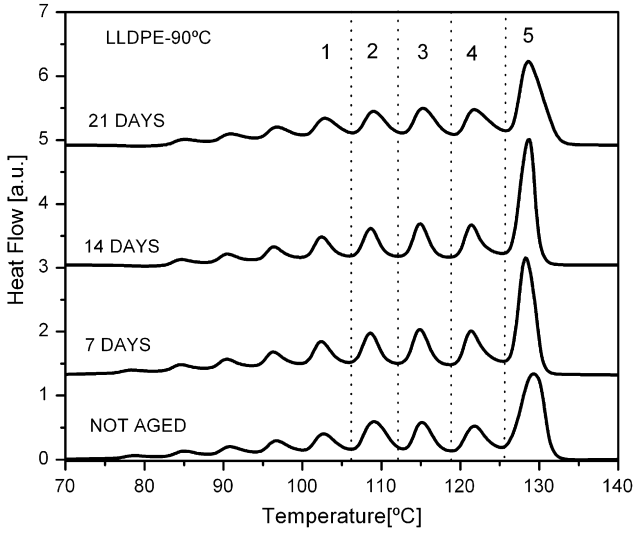

Fig. 3. DSC melting runs for LLDPE-AF for several values of aging time, at 90 °C.

Table 1
Areas fractions for each DSC scan shown in Fig. 1 for several self-seeding temperature (T_s) and degradation temperatures

Partial area fractions (21 days)						
T_s (°C)	Peak no.	Not aged	LDPE-AF			LDPE
			60	75	90	90
119	4				0.055	0.019
113	3	0.18	0.26	0.31	0.37	0.315
107	2	0.31	0.295	0.29	0.315	0.30
101	1	0.17	0.17	0.175	0.11	0.15
95		0.11	0.115	0.0115	0.07	0.086
89		0.08	0.075	0.075	0.05	0.059

The chain scission process may free polymethylene chain ends and allow the increase of the formation of lamellae that melt at peak 3 temperature. If the cause for the increase of area under peak 3 is associated with the oxidative aging in air, this must not be used to compare reaction rates for chain scission and crosslinking, since low crosslinking levels will not have much influence on the controlled crystallization processes [27,28]. Fig. 2 shows the final DSC melting runs for LDPE-AF for several values of aging time, at 90 °C. The values of area fractions are also shown in Table 2, for a more quantitative evaluation of the aging evolution at the shorter times where data are available. For the sample aged for 7 days, we observe that the area under peak 3 increases, almost in the same amount as peak 2 decreases. The peak 3 melting temperature corresponds to lamellae of thickness of about 75 Å, while the peak 2 melting temperature corresponds to lamellae about 62 Å thick, calculated from the Gibbs–Thomson equation [19,21,29,30]. Tertiary carbon atoms in the amorphous solid state are linked to at least one amorphous chain length about 5–10 methylenes long. Chain scission of a tertiary carbon atom neighboring chains that melt under peak 2 may well free at least one length of polymethylene chain that can now crystallize in thicker lamellae that correspond to peak 3.

Table 2
Area fractions for each DSC scan in Figs. 2 and 3 for several self-seeding temperatures (T_s) and aging days

Material	Partial area fractions							
	T_s (°C)	Peak no.	Days					
			Not aged	7	14	21	28	43
LDPE-AF, 90 °C	*119*	4			0.025	0.055	0.04	
	113	3	0.18	0.305	0.32	0.37	0.39	0.52
	107	2	0.31	0.22	0.31	0.31	0.29	0.245
	101	1	0.17	0.17	0.145	0.11	0.105	0.09
	95		0.11	0.11	0.095	0.07	0.065	0.05
	89		0.08	0.075	0.065	0.05	0.045	0.03
LLDPE-AF, 90 °C	*125*	5	0.28	0.28	0.33	0.32	0.31	0.29
	119	4	0.115	0.14	0.135	0.14	0.155	0.135
	113	3	0.11	0.125	0.135	0.14	0.14	0.13
	107	2	0.14	0.12	0.125	0.13	0.13	0.125
	101	1	0.095	0.105	0.11	0.11	0.11	0.115
	95		0.075	0.085	0.075	0.07	0.075	0.08
	89		0.055	0.055	0.05	0.05	0.05	0.06

For peaks 1 and 2, Figs. 1 and 2 show similar evolutions in time, but quantitative tracking is now much more complicated, since these may conceivably change due to simultaneous processes of chain scission and crosslinking. Following the above reasoning, chain scission would increase thicker lamellae content, while crosslinking effect would involve a decrease of thicker lamellae content with some increase of thinner lamellae.

A somewhat unexpected result is the appearance and growth of peak 4, which can also be seen in Fig. 1 for the sample aged at 90 °C. Peak 4 shows up after aging for 14 days at 90 °C, and grows with time, and may also develop as a consequence of tertiary carbon scission. The appearance of peak 4 ought to be expected at the later degradation stages, because the content of longer polymethylene crystallizable sequences is scarce for this type of polyethylene.

Fig. 3 shows the final DSC melting runs for LLDPE-AF for several values of aging time, at 90 °C. The temperature range encompassed by the melting peaks is higher and wider than for the LDPE samples, due to the different distribution of tertiary carbon atoms in the not aged polymer. Peaks 4 and 5 are now always present. Peaks 3, 4 and 5 change slightly along aging time, but we have not been able to find easy and accurate ways to correlate the changes seen in SSA results with results from other experimental techniques. Peak 5 increases in height first, and then widens, and similar smaller changes are observed for others. These results are quantified in Table 2. Looking for reasons for this behavior, we pay attention first to peak 5, and compare with results obtained for peak 3. A simple calculation – via the well-known Gibbs–Thompson equation – shows that peak 3 is placed in a temperature region where changes of 10–15 Å in lamellae thickness correspond to changes of about 5–8 °C of melting temperature. Similar changes of 10–15 Å in lamellae thickness in the peak 5 temperature range would not be noticed by SSA, since the expected melting temperature changes would be of about 1–2 °C; and only minor changes like peak widening would be observed. For the LLDPE, peaks placed at temperatures lower than peak 5 suffer the same difficulties as do peaks 1 and 2 for LDPE samples, described above.

We understand that the use of SSA for early polyolefin degradation is best suited for the case of LDPE tertiary carbon distribution along the main chains.

Fig. 4 shows a comparison of results from SSA peak 3 evolution and FTIR determination of carbonyl concentration. Carbonyl concentrations (w/w) were measured for samples aged at 90 °C for 0, 7, 28 and 43 days, and these numbers are shown on the right side of the graph. The increase of the area fraction under peak 3 was determined from SSA results for the same samples, at 90 °C, aged for 7, 14, 21, 28, and 43 days, and shown on the left side of the graph. Within some scatter, a linear correlation is found between carbonyl concentration content and peak 3 area fraction changes.

Table 1 shows also a column of SSA area fraction data for a LDPE sample that was not washed with the before mentioned procedure, and thus contained all the original additives, including antioxidants, aged at 90 °C. Data show that similar

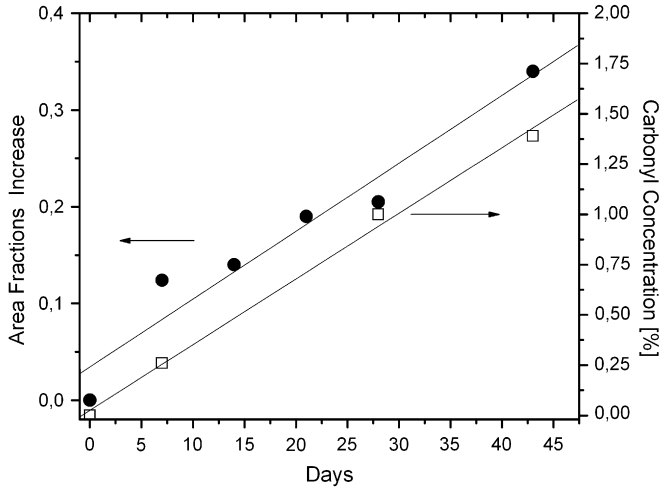

Fig. 4. Comparison of results from SSA peak 3 evolution and from FTIR.

results were obtained, and the antioxidant delayed the degradation process.

Fig. 5 shows the final DSC melting runs for three samples: not aged LDPE (203M), a sample extracted from a pipeline liner section for which the mechanical behavior was ductile, and another sample extracted from a pipeline liner section for which the mechanical behavior was fragile. Changes observed for the fragile LDPE liner peaks labeled 2 and 3 agree with changes shown in Fig. 2. Oxidative degradation causes peak 3 for the fragile liner sample to grow, while the corresponding peak 2 is reduced. Much smaller changes are observed for peaks 2 and 3 for the liner sample taken from the section that still remains ductile, that can be observed when compared with results for the not aged LDPE (203M). Oxidative degradation for the ductile liner section is much less than for the fragile liner section.

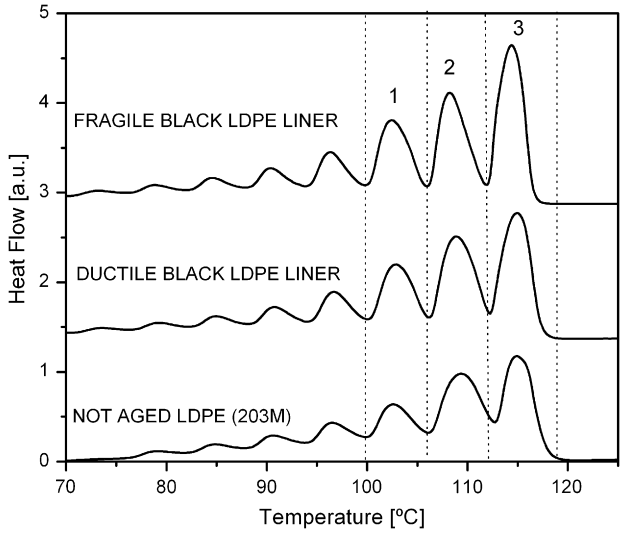

Fig. 5. DSC melting runs for not aged LDPE (203M), ductile black LDPE liner and fragile black LDPE liner, after SSA treatment.

4. Conclusions

The development of the area fractions for the SSA melting peak 3, located at 114 °C, correlates linearly with the amount of carbonyl groups measured by FTIR. The sensitivity of the method proposed is similar to the sensitivity of FTIR, for melting peaks located near 114 °C. Other melting peaks located at higher temperatures exhibit lower sensitivity. Peaks located at lower temperatures should not be expected to correlate linearly with carbonyl group formation, for reasons discussed above. The proposed SSA technique looks very promising to be used for the monitoring of early LDPE degradation processes. Other polyethylene types melt in temperature ranges that are less sensitive to the changes in the features of lamellae thickness.

Acknowledgements

The authors acknowledged to the National Research Council of Argentina (CONICET) and ANPCyT (Project FONCyT-PICT03-12-14570) for the financial support.

References

[1] Hassinen J, Lundbäck M, Ifwarson M, Gedde UW. Polym. Degrad Stab 2004;84:261–7.
[2] Gulmine JV, Janissek PR, Heise HM, Akcelrud L. Polym Degrad Stab 2003;79:385–97.
[3] Ohtake Y, Kobayashi T, Asabe H, Murakami N, Ono K. J Appl Polym Sci 1995;56:1789–96.
[4] Ohtake Y, Kobayashi T, Asabe H, Murakami N, Ono K. J Appl Polym Sci 1998;70:1643–8.
[5] Gedde U, Ifwarson M. Polym Eng Sci 1990;30:202–10.
[6] Gugumus F. Polym Degrad Stab 1999;66:161–72.
[7] Gugumus F. Polym Degrad Stab 2000;68:219–22.
[8] Gugumus F. Polym Degrad Stab 2001;74:327–39.
[9] Khelidj N, Colin X, Audouin L, Verdu J, Monchy-Leroy C, Prunier V. Polym Degrad Stab 2006;91:1598–605.
[10] Pinheiro LA, Chinelatto MA, Canevarolo SV. Polym Degrad Stab 2006;91:2234–332.
[11] Chiellini E, Corti A, D'Antone S, Baciu R. Polym Degrad Stab 2006;91:2739–47.
[12] Iring M, Tüdös F. Prog Polym Sci 1990;15:217–62.
[13] Hoang M, Allen NS, Liauw CM, Fontán E, Lafuente P. Polym Degrad Stab 2006;91:1356–62.
[14] Corrales T, Catalina F, Peinado C, Allen NS, Montan E. J Photochem Photobiol A 2002;147:213–24.
[15] Do TT, Celina M, Fredericks PM. Polym Degrad Stab 2002;77:417–22.
[16] Delor F, Lacoste J, Barrois-Oudin N, Cardinet C, Lemaire J. Polym Degrad Stab 2000;67:469–77.
[17] Delor F, Lacoste J, Lemaire J, Barrois-Oudin N, Cardinet C. Polym Degrad Stab 1996;53:361–9.
[18] Müller AJ, Hernández ZH, Arnal ML, Sánchez JJ. Polym Bull 1997;39:465–72.
[19] Arnal ML, Balsamo V, Ronca G, Sánchez A, Müller AJ, Cañizales E, et al. J Therm Anal Calorim 2000;59:451–70.
[20] Marquez L, Rivero I, Müller AJ. Macromol Chem Phys 1999;200:330–7.
[21] Müller AJ, Arnal ML. Prog Polym Sci 2005;30:559–603.
[22] Fillon B, Thierry A, Wittmann J, Lotz B, Thierry A. J Polym Sci Part B Polym Phys 1993;31:1383–93.
[23] Bikiaris D, Prinos J, Panayiotou C. Polym Degrad Stab 1997;56:1–9.

[24] Briassoulis D, Aristopoulou A, Bonora M, Verlodt I. Biosyst Eng 2004;88:131–43.
[25] Paolini Y, Ronca G, Feijoo JL, Da Silva E, Ramírez J, Müller AJ. Macromol Chem Phys 2001;202:1539–47.
[26] Pérez CJ. Doctoral thesis. Universidad Nacional del Sur, Bahía Blanca, Argentina; 2003.
[27] Pérez CJ, Villarreal N, Pastor JM. VII Simposio Argentino de Polímeros, III Simposio Binacional Argentino-Chileno, Córdoba, Diciembre; 2005.
[28] Pérez CJ, Failla MD, Vallés EM. Polymer 2005;46:725–33.
[29] Virkkunen V, Laari P, Pitkanen P, Sundholm F. Polymer 2004;45:4623–31.
[30] Alonso M, Rodriguez-Cabello JC, Merino JC, Pastor JM. Macromol Chem Phys 1996;197:3269–84.